

# Ultrasonically tissue-mimicking liver including the frequency dependence of backscatter

Ernest L. Madsen, James A. Zagzebski, Michael F. Insana, Thomas M. Burke, and Gary Frank

Medical Physics Department, University of Wisconsin, Madison, Wisconsin 53706

(Received 26 January 1982; accepted for publication 22 April 1982)

Tissue-mimicking (TM) liver, previously reported by our laboratory, mimics the speed of sound, density, and attenuation coefficient (including frequency dependence) of liver; however, scatter properties are only qualitatively simulated. Two new versions of TM liver are reported here which not only mimic liver with respect to speed of sound, density, and attenuation coefficient, but also with respect to backscatter coefficients, including the frequency dependence of the latter. Compositions, methods of production, and comparisons of ultrasonic properties with those found in the literature for human liver are presented.

Key words: ultrasonic, diagnostic, tissue-mimicking phantom, backscatter

## INTRODUCTION

Previously described gelatin-based ultrasonically tissue-mimicking (TM) materials<sup>1,2</sup> are capable of matching the speed of sound, density, and attenuation coefficient (including the frequency dependence) of liver. Ultrasonic scatter is simulated in only a limited way. In order for a material to be truly equivalent to liver ultrasonically, it should also possess the same differential scattering cross section per unit volume  $\sigma_v(\theta)$  as that of liver for all diagnostic frequencies and all scattering angles  $\theta$ .

A new technique has been developed for production of TM materials, which should lead to the quantitative matching of  $\sigma_v(\theta)$  for liver and other tissue parenchymae. Unfortunately, quantitative data for  $\sigma_v(\theta)$  is not yet available in the literature for all angles  $\theta$  for liver or any other tissue parenchyma. The scattering data which is available is that for backscatter coefficients, defined as  $\sigma_v(\theta)$  for  $\theta = 180^\circ$ . Thus, at present, the scatter properties of new TM liver materials can be quantitatively compared with those of liver only in terms of measured backscatter coefficients. The frequency dependence of the backscatter coefficient for the previously reported gelatin-based TM materials is too great to match that of liver in the diagnostic range. The backscatter coefficients exhibit an approximately  $f^n$  dependence for the frequency range 1–8 MHz where  $3.5 < n \leq 4$ .<sup>3</sup> It is likely that the scatterers involved are individual graphite particles having diameters in the range 40 to 60  $\mu$ . According to Bamber and Hill<sup>4</sup> and Nicholas,<sup>5</sup> no such large frequency dependence exists for human liver, particularly at lower diagnostic frequencies. Their data suggest that, between 1 and 2 MHz, the backscatter coefficient is nearly constant and, above 2 MHz, increases with an apparently increasing rate with frequency.

Nicholas<sup>6</sup> has proposed a model for liver, based in part on the microscopic structure of human liver, consisting of two sets of scatterers: one set having separations of about 1 mm and another set having diameters much smaller than the diagnostic ultrasound wavelengths. Liver actually does consist of a connective tissue matrix in which clumps of cells are distributed, these clumps being about 1 mm in diameter.

Thus, the above anatomical model appears to serve as a useful starting point for production of TM material which mimics liver quantitatively with respect to scatter. In this paper, we report on two new versions of TM liver conforming to this idea of two such sources of scatter. Both versions consist of closely packed agar spheres having diameters between 1.2 and 1.7 mm, with the intervening matrix being filled with a material having a higher density and higher speed of sound consisting of a suspension of microscopic graphite particles in animal hide gel. The significant small particle scatterers in each TM material consist of graphite particles ranging from 40 to 90  $\mu$  in diameter. In one version, these small particle scatterers are randomly distributed in the agar spheres and in the other, they are randomly distributed in the matrix material. There are two reasons for the two versions: one is to determine which is the easiest to produce and the other is to find out if any differences are seen in ultrasonic properties based only on whether the small particle scatterers are inside the agar spheres (simulating clumps of cells) or inside the matrix material (simulating the connective tissue matrix in liver). Both of these TM materials were found to mimic liver in terms of speed of sound, density, and attenuation coefficient as a function of frequency. Both also mimic liver with respect to available measurements for the frequency dependence of their backscatter coefficients.

Of considerable practical importance is the fact that the agar and animal-hide gel components of these materials have been shown to be stable for years and to have melting points in excess of 68  $^\circ\text{C}$ .<sup>2,7,8</sup>

Measurements on the new TM liver versions of speeds of sound, densities, attenuation coefficients, and backscatter coefficients are reported here. In addition, preliminary data on differential scattering cross sections per unit volume are displayed for a range of frequencies and scattering angles. These measurements are of interest for two reasons. One is to gain a better understanding of the scattering mechanisms of these materials (which should be similar to those of liver), and the second reason is to see if any evidence of angular dependent Bragg scattering is present. Attempts to observe such Bragg scattering effects in liver tissue have been report-

ed.<sup>9,10</sup> Detection of Bragg scattering effects in the TM materials would add support to claims that these effects might eventually be useful as diagnostic tools.

## COMPOSITION

The agar spheres are in close contact with one another. The intervening higher density, higher speed of sound matrix consists of a version of TM materials previously reported.<sup>7</sup> This matrix material consists of a macroscopically uniform suspension of graphite particles in an animal hide type gelatin. The concentration of graphite powder in the matrix material is rather high, being 0.22 gm/cm<sup>3</sup>.

### TM liver A

In this case, the matrix material contains graphite powder, the maximum particle size diameter of which is about 22  $\mu$ . The contribution—by scatterers in this matrix material—to the backscatter coefficient for the composite material is negligible. Significant small-particle contributions to scattering should arise from the larger graphite particles randomly distributed within the agar spheres. The latter particles, though low in concentration (0.0105 gm/cc), consist of graphite particles almost exclusively in the 40 to 90- $\mu$ -diam range.

### TM liver B

In this form of TM liver, no small particle scatterers exist in the agar spheres. Instead, the graphite powder in the matrix material contains particles ranging in diameter from 0.1 through 90  $\mu$ ; thus, small particle scattering should arise from within the matrix material.

## METHODS OF PRODUCTION (patent pending)

### The agar spheres

The agar spheres were mass-produced at the rate of about 2 liters/hour using the technique described below.

The basic idea involved is that of the "shot tower" used during the early days of the production of gun shot. In this case, the spheres formed are agar instead of lead, and the medium through which the congealing spheres fall is a kerosene-oil solution instead of air. The shot tower used is about 1 m high and is filled with the kerosene-oil solution. The upper section of the kerosene-oil solution is held at a temperature which exceeds the congealing temperature of the molten agar, and the lower section at a temperature of about 0 °C. These temperatures are maintained by one jacket, containing circulating hot water, surrounding the upper region and another jacket, containing ice water, surrounding the remaining lower part of the shot tower. Aluminum heat exchange tubes are also present.

Molten agar, containing any desired suspended particles, is ejected through a rotating "shower head" near the top of the tower, the agar forming into droplets the size distribution of which depends on the rate of rotation of the shower head. Uniformity of the concentration of suspended graphite particles inside the ejected small droplets is assured through agitation devices in the supply reservoir from which the shower head is supplied with molten agar. The agar droplets

are ejected into the hot kerosene-oil solution by the shower head immediately form into liquid spheres and descend through the less dense kerosene-oil. It takes only a few seconds for these liquid spheres to descend to the lower temperature region of the kerosene-oil column. Since the congealing temperature of the agar is 38 °C, the spheres likely congeal seconds after reaching the top of the lower temperature region. The distance from the shower head to the top of the lower temperature kerosene-oil region is about 15 cm; thus, most of the 1-m length of the column consists of low-temperature kerosene-oil. The reason for this is that the apparatus can also be used to produce much larger spheres (up to about 6 mm in diameter) and these require a longer congealing time and, hence, a longer low temperature section.

There was some concern that the larger graphite particles suspended in the agar spheres to be used in the TM liver A would not be spatially randomly distributed due to gravitational effects before congealing. However, the graphite particles in the agar spheres can be seen as individual particles with a magnifying glass and, no particle concentration gradients being detectable, the particles are presumably randomly distributed.

The congealed spheres are easily removed from the kerosene-oil solution by taking advantage of the fact that they are not only more dense than the kerosene-oil solution, but are more dense than water. Thus, the kerosene-oil solution can be "floated" away from the spheres by addition of water. The spheres can then be stored in a 5% *n*-propanol, 0.5% HCHO aqueous solution. The spheres are also at some point sieved into fractions according to diameter. This sieving is done using the aqueous solution described above.

### Introduction of the matrix material

It is necessary to achieve an adequate difference in density and/or compressibility between the agar spheres and the surrounding matrix in order for significant scattering—related to the boundaries of the agar spheres—to occur. This is achieved by draining the aqueous solution from the agar spheres, and adding a sufficient amount of them to the molten matrix material. The volume of molten matrix material used is three times the total volume of the spheres plus any aqueous solution clinging to the spheres after draining. The use of this much larger volume of molten matrix material than appears necessary is done to offset the diluting effect of any such residual aqueous solution which clings to the spheres following the draining. The spheres and matrix material are stirred well so that any such diluting effect is uniform throughout the molten matrix material. Then an adequate amount of formaldehyde is added to insure that the matrix material will have a melting point exceeding 70 °C following congealing.<sup>7</sup> The congealing takes at least 30 min. For the first 5 min following addition of the formalin, the mix is slowly stirred with a vertically held rod to speed the flotation and resulting close packing of the agar spheres in the more dense molten matrix material.

Next, the uppermost slurry consisting of the agar spheres in molten matrix material is used to make test objects. First a 19-mm-diam spherical test object is formed by closing a two-part spherical mold while immersed in the material. Then part of the remaining material is introduced into a 5 cm long,

7.6 cm in diameter, cylindrical test object. The parallel flat ends of this cylinder are covered with 50- $\mu$ -thick Saran Wrap (Saran Wrap is the trade name for a vinylidene chloride-vinyl chloride copolymer manufactured by the Dow Chemical Co., Midland, MI). The freshly filled test cylinder is then sealed so that the slurry contained makes no contact with air. The test cylinder and the filled spherical mold are then rotated at 2 rpm about a horizontal axis as insurance against gravitationally induced sedimentation during the remainder of the molten state. Finally, the remaining agar spheres floating in the molten matrix material are removed with a spoon and the pure matrix material is poured into a test cylinder such as that described above.

The cylindrical test cylinders are used to make measurements of attenuation coefficients, speeds of sound and backscatter coefficients of the TM materials.<sup>1,3</sup> The 19-mm-diam spherical samples were used to make measurements of differential scattering cross sections.

## MEASUREMENT OF ULTRASONIC PROPERTIES

All measurements were done at 22 °C, a typical room temperature.

### Speeds of sound and attenuation coefficients

Measurements of speeds of sound and attenuation coefficients were done using a through-transmission technique involving displacement of distilled water by the cylindrical test cylinders. This technique has been described previously.<sup>1</sup>

### Backscatter coefficients

Backscatter coefficients were measured using the technique of Sigelmann and Reid,<sup>11</sup> modified by placing the planar reflector, which gives rise to the reference signal, at a distance from the interrogating transducer equal to one-half the distance between the transducer and the interrogated volume of scatterers.<sup>3</sup> This modification may result in an improved representation of the beam intensity incident on the interrogated scattering volume, based on the definition of backscatter coefficient.

Three 13-mm-diam nonfocused transducers were used at a distance of 20 cm from the gated interrogated region. At each sample position nine data points were obtained as the transducer was translated laterally in 6-mm increments over a 12  $\times$  12-mm grid. Between sets of nine observations, the sample was translated axially along the beam so that the total sample depth interrogated was about 2.5 cm. For each sample and frequency, at least 27 data points were obtained. On the basis of the smoothness of the frequency dependence of the data obtained, the volume interrogated appears to have been sufficiently large to avoid significant influence of local fluctuations in spatial regularity.

### Differential scattering cross sections as functions of scattering angle

Differential scattering cross sections per unit volume  $\sigma_v(\theta)$  were measured for scattering angles between 34.6° and 175.0° (nearly backscatter) in 3.6° increments using a method described elsewhere.<sup>12</sup> Basically, this involves placing the 19-mm-diam sphere of TM material in the very far field of a

source transducer (a distance of about 60 cm) and recording the scattered signals with a receiving transducer at a comparable distance from the sphere. For each frequency and scattering angle, the signal is recorded for 150 angular orientations of the spherical scattering volume as the latter is rotated about an axis perpendicular to the scattering plane involved in the measurements. The data represent averages for these orientations; the total angle through which the sphere is rotated is 360°. The reference signal, representing the amplitude incident on the sphere, is found by recording the peaked response of the receiver when placed at the position of the sphere, the sphere being removed. Continuous wave (cw) bursts are employed which are of sufficient duration that the part of the scattered signal monitored results from incident plane sinusoidal waves only; i.e., the onset and termination of the cw bursts are not factors.

### Density determination

Densities were determined in a direct fashion involving volume and mass measurements of a graduated cylinder partially filled with water. The water level and total mass were measured before and after immersion of about 50 g of the TM material in the water. Density is considered to be an ultrasonic property of importance when more than one TM material are included in a phantom and interfaces exist between different TM materials.

## RESULTS, ERROR DISCUSSION, AND COMPARISON WITH DATA FOR NORMAL HUMAN LIVER

### Attenuation coefficients, speeds of sound, and densities

Figures 1–5 contain graphs of measured attenuation coefficients  $\alpha$  at eight frequencies between 1.00 and 8.00 MHz. Also shown in each figure are the speed of sound  $c$  at 2.00 MHz and the result of a curve-fitting analysis for  $\alpha$ . Figures 1–4 correspond, in order, to TM liver A, the matrix material for TM liver A, TM liver B, and the matrix material for TM liver B. Figure 5 corresponds to a special test cylinder made

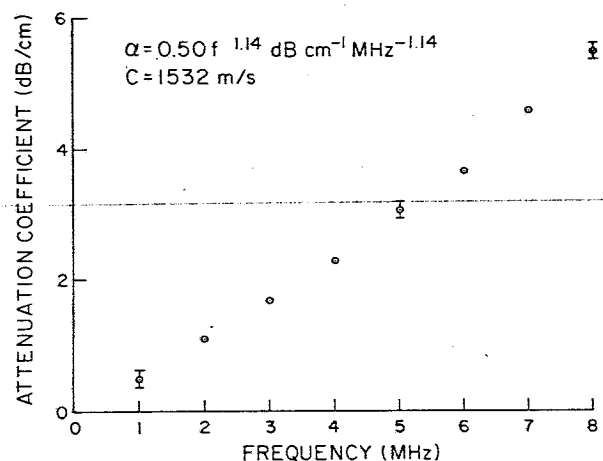


FIG. 1. Attenuation coefficients at eight frequencies for TM liver A. The speed of sound at 2.00 MHz is shown also, as well as the result of a curve-fitting analysis for the attenuation coefficients. The error bars represent instrumental uncertainties.

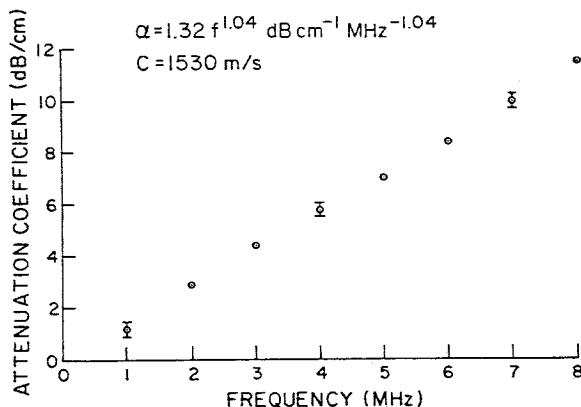


FIG. 2. Attenuation coefficients at eight frequencies for the matrix material of TM liver A. The result of a curve fitting analysis of the data is shown, as well as the speed of sound at 2.00 MHz. The error bars represent instrumental uncertainties.

up of closely packed (but not distorted from their spherical shape) agar spheres having diameters 1.70 through 2.36 mm; these spheres contain the same distribution of larger graphite particles which are contained in the smaller agar spheres of TM liver A. The purpose of these measurements was to gain some insight into the extent of the contribution to the total attenuation of TM liver A of the internal components of the agar spheres. Also of interest is the speed of sound value compared to that of the matrix material. The latter information, together with the values of densities in the spheres and in the matrix material, will be useful in understanding the nature of the intermediate particle scattering. The error bars on the attenuation coefficients and uncertainties in speeds of sound (see Table I for uncertainties in speeds of sound) result from instrumental uncertainties and the details of the error analyses have been treated thoroughly elsewhere.<sup>8</sup>

Table I shows the values of densities and speeds of sound and their uncertainties for the five materials discussed in the last paragraph. Also given are values for  $\alpha_0$  and  $n$ , assuming that the attenuation coefficients  $\alpha$  can be expressed as functions of the frequency  $f$  in the form  $\alpha = \alpha_0 f^n$ , where  $\alpha_0$

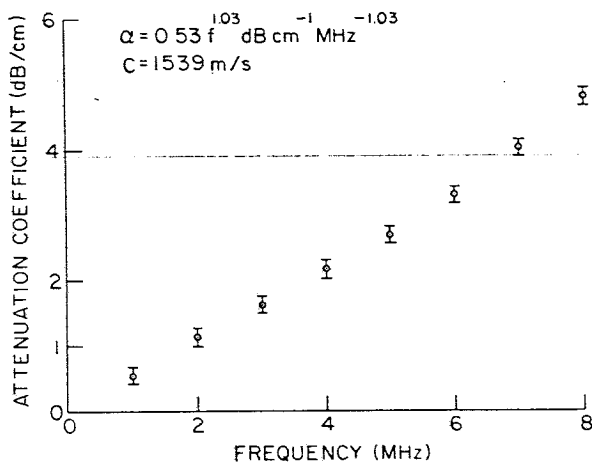


FIG. 3. Attenuation coefficients at eight frequencies for TM liver B. The result of a curve-fitting analysis of the data is shown as well as the speed of sound at 2.00 MHz. The error bars represent instrumental uncertainties.

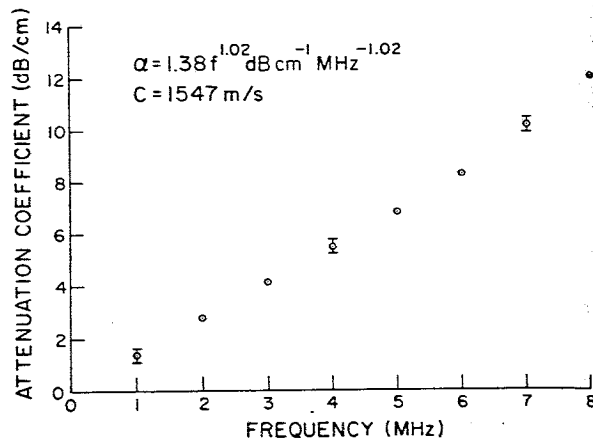


FIG. 4. Attenuation coefficients at eight frequencies for the matrix material of TM liver B. The result of a curve-fitting analysis of the data is shown, as well as the speed of sound at 2.00 MHz. The error bars represent instrumental uncertainties.

and  $n$  are constants.  $\alpha_0$  and  $n$  are obtained via a linear regression analysis applied to  $\ln \alpha = n \ln f + \ln \alpha_0$ . The uncertainties in  $n$  and  $\ln \alpha_0$  (and, therefore, in  $\alpha_0$ ) depend upon the uncertainties in values for  $\ln \alpha$ , which vary considerably over the range of  $\ln \alpha$ . The uncertainties in  $n$  and  $\alpha_0$  were determined via a method described in Bevington.<sup>13</sup>

That the attenuation coefficient for normal human liver is nearly proportional to the frequency has been reported by many investigators.<sup>4,5,14-16</sup> Regarding the slope of the attenuation coefficient, *in vitro* reports usually give values in the range 0.7 to 1.0 dB/cm/MHz. Kuc and Taylor,<sup>16</sup> using a broad band *in vivo* technique, obtained an average attenuation coefficient slope for normal livers of 0.45 dB/cm/MHz. McWhirt *et al.*,<sup>17</sup> using a narrow band *in vivo* tech-

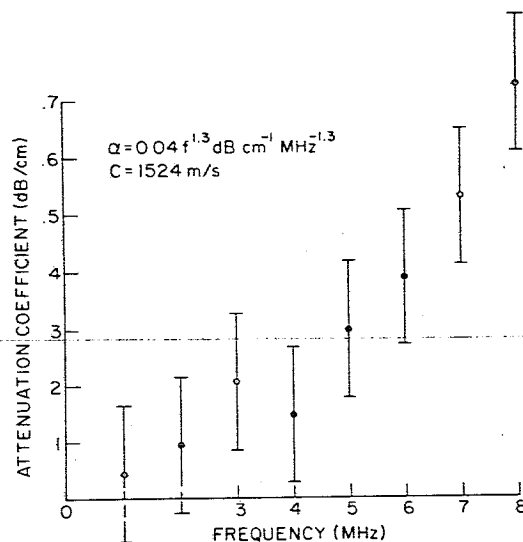


FIG. 5. Attenuation coefficients at eight frequencies for a material consisting of agar spheres, ranging in diameter from 1.70–2.36 mm, suspended in closely packed form in an aqueous medium. The agar spheres contain the same concentration and diameter distribution of graphite particles which are found in the agar spheres of TM liver A. The result of a curve-fitting analysis of the data is shown as well as the speed of sound at 2.00 MHz. The error bars represent instrumental uncertainties.

TABLE I. Summary of ultrasonic properties, not including scatter, for TM livers A and B and for some component materials. The attenuation coefficients were assumed to have the form  $\alpha = \alpha_0 f^n$ , where  $\alpha_0$  and  $n$  are constants and  $f$  is the frequency.

Material	TM liver A	Matrix of TM liver A	Agar spheres of TM liver A in aqueous solution	TM liver B	Matrix of TM liver B	Agar in spheres of TM liver B
$\alpha_0$ (dB cm <sup>-1</sup> MHz <sup>-n</sup> )	0.50 $\pm$ 0.04	1.32 $\pm$ 0.10	0.04 $\pm$ 0.03	0.53 $\pm$ 0.05	1.38 $\pm$ 0.10	0.05 $\pm$ 0.05
$n$	1.14 $\pm$ 0.04	1.04 $\pm$ 0.04	1.3 $\pm$ 0.4	1.03 $\pm$ 0.04	1.02 $\pm$ 0.04	1.1 $\pm$ 0.4
Speed of sound (m s <sup>-1</sup> )	1532 $\pm$ 1	1530 $\pm$ 1	1524 $\pm$ 1	1539 $\pm$ 1	1547 $\pm$ 1	1524 $\pm$ 1
Density (gm cm <sup>-3</sup> )	1.048 $\pm$ 0.005	1.138 $\pm$ 0.005	1.010 $\pm$ 0.005	1.058 $\pm$ 0.005	1.140 $\pm$ 0.005	1.005 $\pm$ 0.005

nique at 3.5 MHz, reported an average value of  $0.5 \pm 0.1$  dB/cm/MHz.

The values for attenuation coefficients obtained for TM livers A and B closely approximate these measurements on human liver, particularly for the *in vivo* data.

Speeds of sound were measured *in vivo* by Mountford and Wells.<sup>18</sup> Their average value was 1540 m/s for normal human liver. Frucht<sup>19,20</sup> averaged speeds of sound measured on 51 samples of freshly excised normal human liver and obtained 1570 m/s; these measurements were done at 24 °C. Bamber and Hill<sup>4</sup> measured speeds of sound at 20 °C on 15 freshly excised normal human livers and obtained an average of 1577 m/s. The speeds of sound for TM livers A and B agree well with the *in vivo* data. The speed of sound in these materials can easily be raised by increasing the concentration of *n*-propanol; e.g., 1580 m/s could easily be attained, if desired.

Values for the densities of TM livers A and B compare quite favorably with the value 1.06 gm/cm<sup>3</sup> given in Wells.<sup>21</sup>

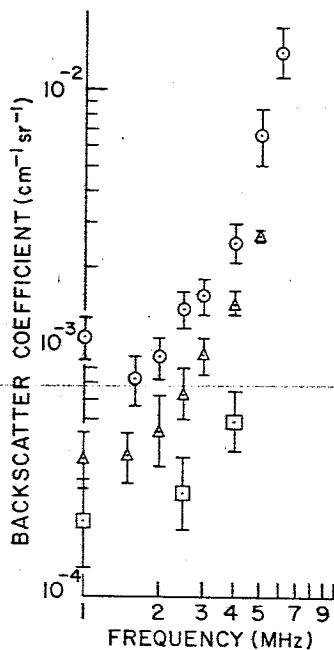


FIG. 6. Mean backscatter coefficients vs frequency for TM liver A (○) and from *in vitro* measurements on normal human liver by Nicholas (Ref. 5) (△) and by Bamber and Hill (Ref. 4) (□). The error bars for the TM liver A data represent standard deviations of the means.

### Backscatter coefficients

Figure 6 shows backscatter coefficients for TM liver A as well as for two sets of data for freshly excised normal human liver. The data for normal human liver were taken from Bamber and Hill<sup>4</sup> and Nicholas.<sup>5</sup> In one case (Nicholas), the data for eight normal excised liver samples were averaged and in the other case (Bamber and Hill) averaging was done for 17 samples. The error bars are referred to as "standard errors of the mean" by Nicholas and simply as "standard errors" by Bamber and Hill. The two sets of *in vitro* data show similar frequency dependencies, viz., a relatively small

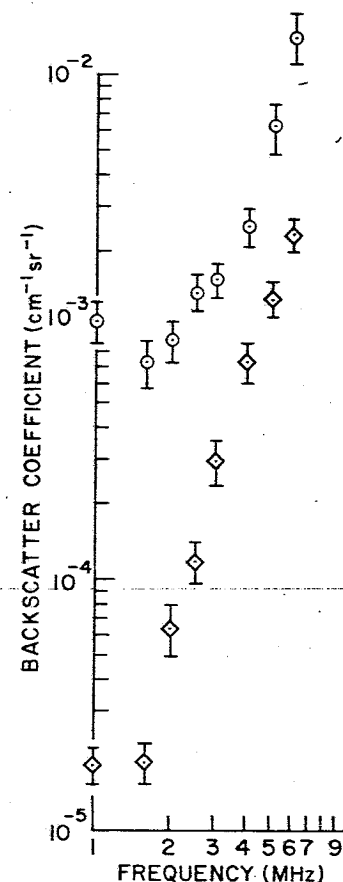


FIG. 7. Mean backscatter coefficients vs frequency for TM liver A (○) and for the material described in the caption of Fig. 5 (◇). The error bars represent standard deviations of the means.

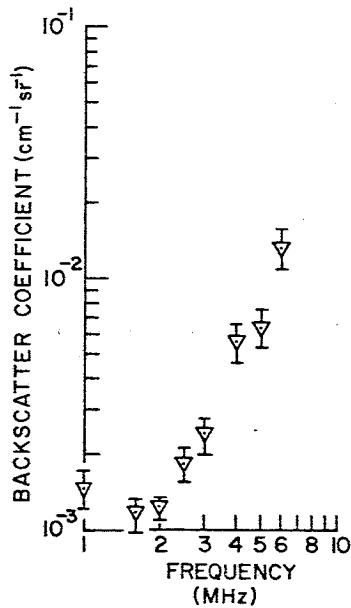


FIG. 8. Mean backscatter coefficients vs frequency for TM liver B done by the method of Insana *et al.* (Ref. 3). The error bars represent standard deviations of the means.

change in backscatter coefficient between 1 and about 2 MHz and then an enhanced frequency dependence above 2 MHz.

The data obtained on TM liver A compare very favorably with the *in vitro* data in terms of frequency dependence and almost equal the data of Nicholas multiplied by a factor of about 2, except at 1 MHz where the factor is about 3. The error bars for the TM liver A data represent standard deviations of the mean.<sup>22</sup>

Figure 7 shows a reproduction of the backscatter data for TM liver A and for the sample containing closely packed, but not distorted, 1.70–2.36-mm-diam agar spheres in an aqueous medium; recall that the latter spheres contain larger graphite scatterers up to about 90  $\mu$  in diameter. As expected, a high-frequency dependence occurs for the latter sample; presumably, the higher frequency dependence of the backscatter coefficients of TM liver A above 3 MHz is related to the presence of such scatterers in the 1.18–1.70-mm-diam agar spheres.

In Figure 8, seven data points correspond to backscatter coefficients measured for TM liver B (in which the larger graphite particles are suspended in the matrix material). Again, the frequency dependence exhibited in the *in vitro* data is well represented. Notice that the values for TM liver B are nearly all higher than those for TM liver A, agreeing with B scans shown in Fig. 11.

#### Differential scattering cross sections per unit volume as functions of angle

Differential scattering cross sections per unit volume  $\sigma_v(\theta)$  for TM liver B are plotted in Fig. 9 for three frequencies and for scattering angles between 34.6° and 175.0° (180° corresponds to backscatter). The data have been corrected for attenuation in the spherical scattering volume. The same type of plot corresponding to a fourth frequency (1.00 MHz) is given in Fig. 10.

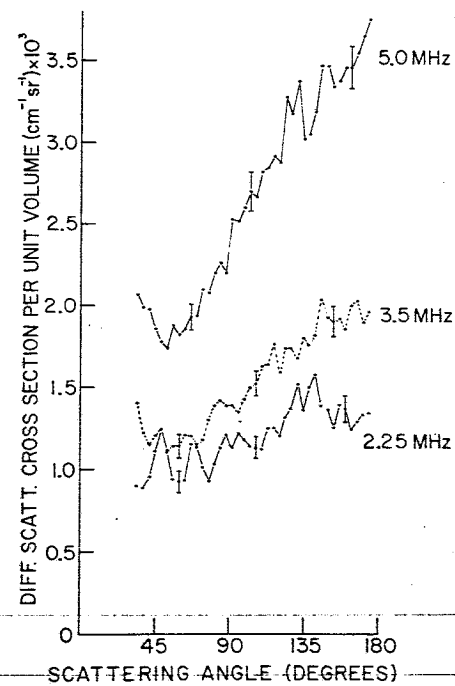


FIG. 9. Mean differential scattering cross sections per unit volume for TM liver B for scattering angles from 36.4° through 175.0° and for ultrasonic frequencies 2.25, 3.50, and 5.00 MHz. The error bars correspond to standard deviations of the means.

#### B scans of TM livers A and B and of the older type of TM liver not containing spherical agar clumps

TM liver developed previously in our laboratory<sup>1,2,7</sup> consists of gels with randomly distributed graphite particles throughout. These particles range in diameter from 0.1 to 90  $\mu$  and are macroscopically uniformly distributed. The latter materials have been found to have backscatter coefficients proportional to  $f^n$ , where  $f$  is the frequency and  $n$  is a constant between 3.5 and 4.<sup>3</sup> Thus, for sufficiently low frequencies, these materials cannot simulate liver with respect to backscatter. This deficiency in the older type TM liver is apparent in the B scans in Fig. 11.

Figures 11(a), (b), (c), and (d) show B scans in which the beam was perpendicular to the Saran Wrap windows of the

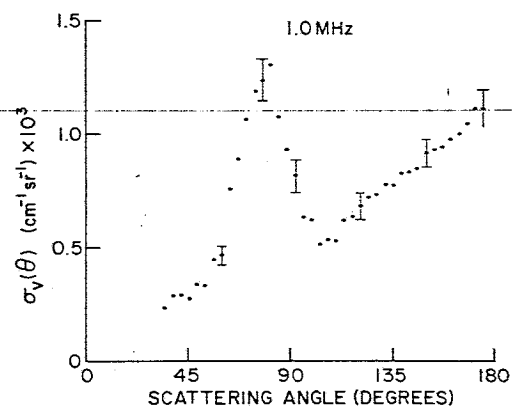


FIG. 10. Mean differential scattering cross sections per unit volume for TM liver B at 1.00 MHz for scattering angles from 36.4° through 175.0°. Error bars refer to standard deviations of the means.

FIG. 11. J  
were scan  
(c), and (

three t  
the sca  
the left  
TM liv  
MHz,  
test cy  
on the  
thick ( case o  
The  
the 5-  
slightl  
of TM  
give r  
A con  
er, ho  
at 2.2  
MHz.

DISC

Bo  
and a  
dence  
for h

Medic

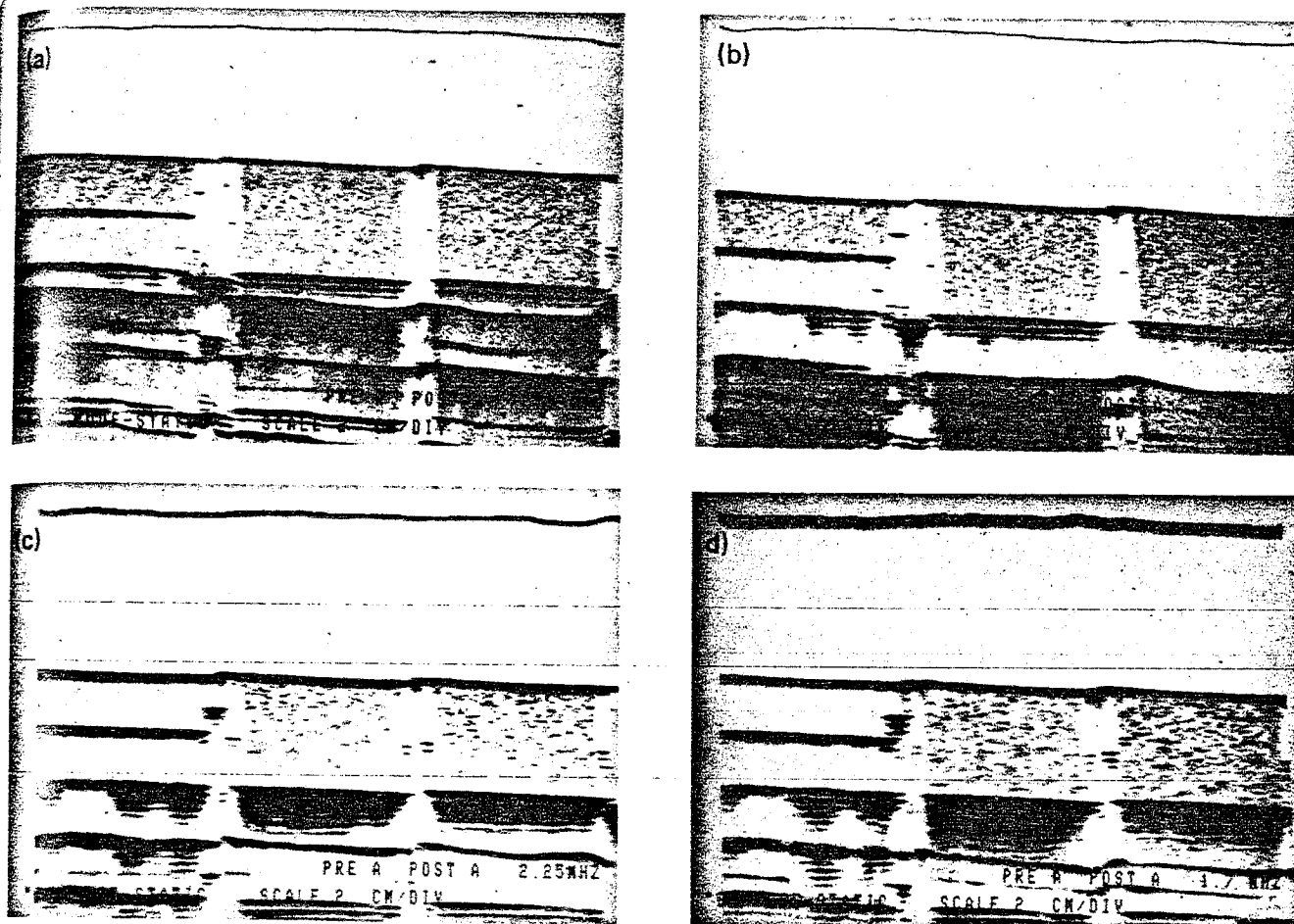


FIG. 11. B scans of the older type TM liver (left-hand side), TM liver A (center) and TM liver B (right-hand side). In each of (a), (b), (c), and (d), all three samples were scanned in the same sweep of the scanning arm, the instrument settings remaining fixed. The nominal frequencies of the scanning transducers in (a), (b), (c), and (d) were, respectively, 5.0, 3.5, 2.25, and 1.6 MHz.

three test cylinders. Respectively, the nominal frequencies of the scanning transducers were 5, 3.5, 2.25, and 1.6 MHz. On the left-hand side is a 2.5-cm-thick cylinder of the older type TM liver, its attenuation coefficient slope being 0.5 dB/cm/MHz, as in the case of TM livers A and B. The TM liver A test cylinder is in the middle and the TM liver B cylinder is on the right—recall that the latter two test cylinders are 5 cm thick (or “deep” in Fig. 11) instead of 2.5 cm thick as in the case of the cylinder containing the older type TM liver.

The distinguishability of the three samples is minimal in the 5-MHz scan. At 3.5 MHz, the older type TM liver has a slightly less bright texture pattern than TM liver A, and that of TM liver B is the brightest. The tendency of TM liver B to give rise to a slightly brighter texture pattern than TM liver A continues through all frequencies. The older type TM liver, however, shows a considerable loss of texture brightness at 2.25 MHz compared to TM livers A and B, and, at 1.6 MHz, its texture pattern is all but absent.

## DISCUSSION AND CONCLUSIONS

Both TM liver A and B exhibit densities, speeds of sound and attenuation coefficients (including the frequency dependence of the latter) which agree well with measured values for human liver, particularly *in vivo* values. They also were

found to have backscatter coefficients which exhibit frequency dependencies very much like those observed in *in vitro* measurements on normal human liver. No *in vivo* measurements of backscatter coefficients are available in the literature. The values at 1 MHz appear slightly higher than desired for agreement with Nicholas' apparently monotonic increase with frequency (Fig. 6). These higher values could be statistical fluctuations considering the extents of the error bars in the lower frequency range (1–3 MHz).

Both types of TM liver were produced relatively easily and possessed very similar ultrasonic properties. In TM liver A, the significant Rayleigh scatterers were in the agar spheres and, in TM liver B, they were in the matrix material between the spheres. The two types, however, exhibit no significant differences in ultrasonic properties, including the frequency dependence of backscatter.

Four tendencies are apparent in the data for differential scattering cross sections per unit volume  $\sigma_v(\theta)$  displayed in Figs. 9 and 10: (1) the increase in  $\sigma_v(\theta)$  with frequency at all scattering angles  $\theta$ ; (2) the increase in  $\sigma_v(\theta)$  with  $\theta$  for a fixed frequency; (3) the greater the frequency, the greater the increase in  $\sigma_v(\theta)$  with  $\theta$ ; and (4) the presence of peaks, particularly the large peak in Fig. 10.

Small peaks for the lesser scattering angles may exist in the data for  $\sigma_v(\theta)$  in Fig. 9 where frequencies 2.25, 3.5, and 5

MHz are represented. However, in Fig. 10,  $\sigma_v(\theta)$  is plotted for 1 MHz and a well-defined strong peak is seen at about  $80^\circ$ . Assuming that short range ordering of the hexagonal close pack type exists in this material<sup>23</sup> and that each agar sphere has an average diameter of 1.45 mm, then the spacing for tetragonal void planes (0.59 mm) is too small to yield a Bragg peak at 1.00 MHz. However, the spacing of the planes for octagonal voids is 1.18 mm (hexagonal close-packed structures have tetragonal and octagonal voids, the number of tetragonal being twice the number of octagonal), and such a spacing corresponds to a Bragg angle of  $80^\circ$ . Thus, evidence for Bragg scattering has come forward. Measurements of  $\sigma_v(\theta)$  for normal animal and human liver are soon to be carried out in our laboratory. Whether strong apparent Bragg scattering can exist in these tissues at it does in TM liver B will be of considerable interest. Results of this study could prompt us to change the diameter distribution of the agar spheres in future TM liver materials.

The above discussion is an example of the value of these new TM materials. The ultrasonic properties of the component materials are known, and the structure is known to within the details of the ordering or lack of ordering of the agar spheres. These materials, while very useful in quality assurance phantoms and in teaching phantoms, may find their greatest value in allowing new diagnostic techniques using ultrasound to be tested on realistic and ultrasonically well characterized materials. In fact, the very discovery of new diagnostic techniques may result from their use.

Regarding control over ultrasonic properties, the speed of sound can easily be raised, if desired, by increasing the concentration of *n*-propanol in the materials. The slope of the attenuation coefficient can be raised without much change in backscatter coefficient by appropriately increasing the concentrations of graphite powder in the matrix material and in the agar spheres. The backscatter coefficient related to intermediate sized scatterers can be increased by increasing the concentration of graphite powder in the matrix material only. (This would increase the slope of the attenuation coefficient also, however.) The backscatter coefficient for intermediate sized scatterers can be decreased without changing the other ultrasonic properties by appropriately increasing the concentration of graphite powder in the agar spheres and reducing the concentration in the matrix. Also, regarding intermediate particle scattering, the diameter distribution of the agar spheres is adjustable in case this distribution is an important parameter.

In the future, varying the speed of sound in the matrix material will probably be desirable in order to match  $\sigma_v(\theta)$  for liver for arbitrary  $\theta$ . Measurements of  $\sigma_v(\theta)$  for liver also must be generated, of course. Such variations of speed of sound in the matrix material can be accomplished by varying the concentration of animal hide gelatin.

## ACKNOWLEDGMENTS

The authors are indebted to Dr. David Nicholas, Dr. J. C. Bamber, and Dr. C. R. Hill, and to Ultrasound in Medicine

and Biology for their permission to allow the reproduction of some of their published data on backscatter coefficients for normal human liver. Gratitude is also expressed to Orlando Canto for his generation of the high-quality figures and to Anne Zimmerman for her typing proficiency. Work supported in part by NCI grants 5-P01-CA-19278 and 5-R01-CA-25634.

- <sup>1</sup>E. L. Madsen, J. A. Zagzebski, R. A. Banjavic, and R. E. Jutila, *Med. Phys.* **5**, 391 (1978).
- <sup>2</sup>M. M. Burlew, E. L. Madsen, J. A. Zagzebski, R. A. Banjavic, and S. Sum, *Radiology* **134**, 517 (1980).
- <sup>3</sup>M. F. Insana, J. A. Zagzebski, and E. L. Madsen, *Med. Phys.* (in press).
- <sup>4</sup>J. C. Bamber and C. R. Hill, *Ultrasound Med. Biol.* **7**, 121 (1981).
- <sup>5</sup>D. Nicholas, *Ultrasound Med. Biol.* **8**, 17 (1982).
- <sup>6</sup>D. Nicholas, "Orientation and frequency dependence of backscattered energy and its clinical application," *Recent Advances in Ultrasound in Biomedicine*, edited by D. N. White (Research Studies, New York, 1977), pp. 29-54.
- <sup>7</sup>E. L. Madsen, "Ultrasonically soft-tissue-mimicking materials," *Medical Physics of CT and Ultrasound: Tissue Imaging and Characterization*, edited by G. D. Fullerton and J. A. Zagzebski (American Institute of Physics, New York, 1980), pp. 531-550.
- <sup>8</sup>E. L. Madsen, J. A. Zagzebski, and G. R. Frank, *Ultrasound Med. Biol.* **8**, 277 (1982).
- <sup>9</sup>R. C. Waag, R. M. Lerner, P. P. K. Lee, and R. Gramiak, "Ultrasonic diffraction characterization of tissue," *Recent Advances in Ultrasound in Biomedicine*, edited by D. N. White (Research Studies, New York, 1977), pp. 87-116.
- <sup>10</sup>P. P. Lele and N. Senapati, "The frequency spectra of energy backscattered and attenuated by normal and abnormal tissue," *Recent advances in Ultrasound in Biomedicine*, edited by D. N. White (Research Studies, New York, 1977), pp. 55-86.
- <sup>11</sup>R. A. Sigelmann and J. M. Reid, *J. Acoust. Soc. Am.* **53**, 1351 (1973).
- <sup>12</sup>T. M. Burke, E. L. Madsen, J. A. Zagzebski, and F. Jafari, "Quantitative measurement of ultrasonic scatter as a function of angle for tissue-mimicking materials," in Proceedings of the Twenty-fifth Annual Convention of the American Institute of Ultrasound in Medicine (September 15-19, 1980, New Orleans, LA), p. 127.
- <sup>13</sup>P. R. Bevington, *Data Reduction and Error Analysis for the Physical Sciences* (McGraw-Hill, New York, 1969), pp. 115-117.
- <sup>14</sup>R. C. Chivers and C. R. Hill, *Ultrasound Med. Biol.* **2**, 25 (1975).
- <sup>15</sup>P. M. Gammel, R. C. Heyser, Le Croisette, J. A. Roseboro, and R. L. Wilson, "The temperature and frequency dependence of ultrasonic attenuation in liver," in Proceedings of the Twenty-third Annual Meeting of the American Institute of Ultrasound in Medicine (October 19-23, 1978, San Diego, CA), p. 128.
- <sup>16</sup>R. Kuc and K. J. W. Taylor, "Progress in characterizing diffuse diseases of the liver using attenuation slope estimates," in Proceedings of the Fifth International Symposium on Ultrasonic Imaging and Tissue Characterization (June 1-6, 1980, Gaithersburg, MD), p. 9.
- <sup>17</sup>R. E. McWhirt, J. Ophir, and N. F. Maklad, "Attenuation coefficient measurements *in vitro* and *in vivo* using a differential C-scan technique," in Proceedings of the Fifth International Symposium on Ultrasonic Imaging and Tissue Characterization (June 1-6, 1980, Gaithersburg, MD), p. 14.
- <sup>18</sup>R. A. Mountford and P. N. T. Wells, *Phys. Med. Biol.* **17**, 14 (1972).
- <sup>19</sup>A. H. Frucht, *Z. Gesamte Exp. Med.* **120**, 526 (1953).
- <sup>20</sup>S. A. Goss, R. L. Johnston, and F. Dunn, *J. Acoust. Soc. Am.* **64**, 423 (1978).
- <sup>21</sup>P. N. T. Wells, *Biomedical Ultrasonics* (Academic, London, 1977), p. 136.
- <sup>22</sup>I. A. Sokolnikoff and R. M. Redheffer, *Mathematics of Physics and Modern Engineering*, 2nd edition (McGraw-Hill, New York, 1966), p. 643.
- <sup>23</sup>L. V. Azaroff, *Introduction to Solids* (McGraw-Hill, New York, 1960), pp. 55-68.

Prope  
meas

## I. INTRO

The dete  
cult pro  
these ar  
radioacti  
and diffi  
Most  
blood flo  
ticular t  
We s  
tion of  
harmon  
tempera  
through  
require

## II. THE

The t  
dimens  
 $\frac{\partial^2 T}{\partial x^2}$   
where  
conduc  
ly. The  
volume  
respect  
the par  
perfuse  
relatio  
flow is  
 $Q =$   
where  
tissue p  
unit vc  
and the  
tissues  
We:  
equatio  
the vic  
viewed  
discus  
the blc